Ravindra Kumar[1], *Ruchika Mehta*[2*], *Deepak Kumar*[1], *Murli Manohar Gaur*[1]

NUMERICAL ANALYSIS OF NANOFLUID FLOW THROUGH MIXED CONVECTIVE NON-LINEAR STRETCHING SHEET INDUCED IN POROUS MEDIA ALONG WITH THERMAL RADIATION

NUMERIČKA ANALIZA STRUJE NANOFLUIDA, KROZ MEŠOVITO KONVEKCIONU NELINEARNO RASTEGLJIVU TRAKU, KOJA SE INDUKUJE U POROZNOJ SREDINI PRI TOPLOTNOM ZRAČENJU

Originalni naučni rad / Original scientific paper
Rad primljen / Paper received: 15.07.2024
https://doi.org/10.69644/ivk-2025-siA-0045

Adresa autora / Author's address:
[1)] Department of Mathematics, Vivekananda Global University, Jaipur, Rajastan, India
[2)] Department of Mathematics & Statistics, Manipal University Jaipur, Rajastan, India *email: ruchika.mehta@gmail.com

Keywords
- nanofluid
- nonlinear stretching sheet
- thermal radiation
- nanoparticle volume fraction
- non-uniform heat source/sink parameters

Ključne reči
- nanofluid
- nelinearno rastegljiva traka
- toplotno zračenje
- zapreminski udeo nanočestica
- parametri neuniformnog izvora/ponora toplote

Abstract

The current research aims to investigate the influence of thermal radiation on heat transfer in a mixed convection nanofluid flow generated by a nonlinear stretching sheet. The study incorporates parameters such as magnetic fields and non-uniform heat source/sink. By employing suitable transformations, nonlinear ordinary differential equations derived from nonlinear Navier-Stokes equations are solved using the Runge-Kutta fourth-order method combined with the shooting method. Graphical representations are utilised to highlight the significance of variables as velocity and temperature. An increase in the Eckert number Ec and the non-uniform heat source/sink parameters (A^*, B^*) leads to enhancements in temperature and velocity. Conversely, higher values of magnetic parameter M, permeability parameter K, and nonlinear stretching parameter n result in decreased velocity and improved temperature distribution. Temperature elevation corresponds to an increase in nanoparticle volume fraction Fi. The Nusselt number and skin friction coefficient exhibit a decreasing trend concerning magnetic restriction M, Prandtl number Pr, permeability restriction K, and nanoparticle volume fraction Fi. Conversely, the skin friction coefficient demonstrates an increasing trend, while the Nusselt number decreases concerning the radiation parameter Ra, non-uniform heat source/sink parameters (A^*, B^*), and the Eckert number Ec.

Izvod

Ovim istraživanjem se izučava uticaj toplotnog zračenja na prenos toplote u mešovitoj konvekcionoj struji nanofluida, koja se generiše nelinearno rastegljivom trakom. Uvode se parametri kojima se opisuju magnetna polja i neuniformni izvor/ponor toplote. Putem odgovarajućih transformacija i primenom Runge-Kuta metode četvrtog reda u kombinaciji sa metodom pogađanja, rešavaju se nelinearne obične diferencijalne jednačine, izvedene iz nelinearnih Navije-Stoksovih jednačina. Iscrtavanjem grafikona se uočava značaj promenljivih, kao što su brzina i temperatura. Porast Ekertovog broja Ec i parametara neuniformnog izvora/ponora toplote (A^*, B^*) doprinosi povećanju temperature i brzine. S druge strane, veće vrednosti magnetnog parametra M, parametra permeabilnosti K i parametra nelinearnog razvlačenja n, doprinosi smanjenju brzine i povećanoj raspodeli temperature. Povećanje temperature odgovara povećanju zapreminskog udela nanočestica Fi. Nuseltov broj i koeficijent trenja na zidu pokazuju smanjenje u odnosu na magnetostrikciju M, Prandtlov broj Pr, permeabilitet K, i zapreminski udeo nanočestica Fi. Suprotno tome, koeficijent trenja na zidu pokazuje trend porasta, dok Nuseltov broj opada s obzirom na parametar zračenja Ra, parametre neuniformnog izvora/ponora toplote (A^*, B^*), i Ekertovog broja Ec.

INTRODUCTION

Xuan and Li /28/ described a method for creating a suspension of nanophase particles in a base liquid called a nanofluid. A numerical analysis has been done to examine the issue of a flat surface being stretched in a nanofluid results in laminar fluid flow, Khan and Pop /15/. The stream and warm transmission of a viscoelastic nanofluid across a stretched surface were explored, considering the impact of viscous dissipation and the additional job required due to warp, Rana and Bhargava /24/. Goyal and Bhargava /7/ examined how a stretched sheet's speed fall border line situation affected the stream and warm transmission of non-Newtonian nanofluids. Consideration is given to the influences of thermophoresis and Brownian motion as well. In Zeeshan et al. /29/, boundaries of natural convection, generating heat using an inverted cone, magnets on different wall temperatures, water and ethylene glycol-based nanofluids are taken into consideration. In Das /2/ a numerical investigation is made into the issue of flow of a nanofluid's boundary layer across a stretching, nonlinear leaky sheet at a certain surface warmth with partial slip. Khan et al. /12/ focused on the 3-dimen-

sional stream of a nanofluid above a flexible pane that has been widened in two asymmetrical directions nonlinearly. In Pal and Mandal /21/, the belongings of thermal rays of varied convective border coating stream towards a stagnation-point stream in nanofluids above an extending or shrinking immersed in spongy media, as well as heat generation and viscous dissipation, are of interest. Sandeep et al. /27/ examined the nanofluid with thermophoretic magnetohydrodynamic dissipative border layer overflow an unstable stretched sheet in a porous material with an internal heat source/sink that varies with space and time. Naramgari and Sulochana /19/ premeditated the mass and heat transport in a thermophoretic radiative nanofluid flowing throughout a sheet immersed in a porous media with internal effects of suction/injection, viscous dissipation, and heat generation/absorption that was increasing exponentially. Das et al. /3/ used Cu-water nanofluid to investigate the convective warmth transport behaviour of nanofluid above a leaky stretched pane with thermal convective border line conditions, a magnetic pasture, slip speed, and how nanoparticles affect flow and heat transfer characteristics. In Devi and Devi /4/, the flow past a stretching sheet is investigated using two fluid types: hybrid nanofluid (Cu-Cl_2O_3/water) and nanofluid (Cu/water). To inspect the influence of physical characteristics, a parametric study has been conducted in Hayat and Nadeem /10/ to increase the rate of heat transmission even more, 'hybrid nanofluid' is being used. This novel 3D model is used to investigate the effects of thermal emission, warm production, and chemical reactions over stretching sheets while rotation is present. Khan and Azam /13/ explored the erratic mass and heat transport mechanisms in a permeable stretching surface-induced magnetohydrodynamic (MHD) Carreau nanofluid flow. In Jamaludin et al. /11/ Cu-water and Ag-water were the two types of nanofluids that were studied in a continuous and porous, vertically expanding/constricting sheet subjected to 3-dimensional MHD mixed convective flow. Malvandi et al. /17/ examined a nonlinear stretching/shrinking sheet under a constant two-dimensional stagnation-point flow of nanofluids in the presence of blowing/suction. In Geng et al. /6/, numerical study is done to study the flow of nanofluids in a rotating system and the transmission of heat between two horizontal plates. Haroun et al. /8/ explored the convective mass and heat transport in a magnetohydrodynamic nanofluid stream through a leaky material in excess of a stretched sheet. (Cu/water) and Al_2O_3/water, two different kinds of nanofluids, are examined. In Patel /22/, convection is blended in two dimensions under the influence of a constant magnetic field, the Casson fluid flows past an infinite serving dish in a spongy medium. Daniel et al. /1/ scrutinize, in the company of heat emission, gooey debauchery, and chemical reactions, the impact of slip circumstances on the electrical magnetohydrodynamic nanofluid flow in a two-dimensional unstable mixed convection flow across a stretched sheet. When nanoparticles and a magnetic field are present, Faraz et al. /5/ explored the phenomena of heat radiation and mixed convection in an axisymmetric flow of Casson fluid. Hayat et al. /9/ studied the effects of buoyancy force on a magnetised, viscoelastic nanofluid. The problem formulation introduces characteristics of Brownian movement, viscous dissipation, and thermophoretic features. Khan et al. /14/ look at the impact of numerous slips on the Jeffrey fluid model for the presence of Soret and radiation in the unstable magnetohydrodynamic viscoelastic buoyant nanofluid in front of a stretched permeable sheet. Nandeppanavar et al. /18/ explore the characteristics of non-Newtonian Casson nanofluid mass and heat transfer in conjunction with steady two-dimensional flow next to the boundary when an exponentially stretching sheet is present. In Roy and Pop /26/, investigations are made into the stream and warm transmission properties of a second-class hybrid nanofluid on a stretchable, leaky sheet. In Mabood et al. /16/, a hybrid nanofluid based on water participating in a consistent, forced convection that evolves on a stretched surface is studied to determine the effect of hybrid nanoparticles on several physical characteristics. In Naveen et al. /20/, the Koo-Kleinstreuer-Li model is primarily used in the study to examine the rheological characteristics of the nanofluids. In Punith Gowda et al. /23/, a theoretical analysis is conducted to investigate the influence of Stefan's blowing condition, thermophoresis, and Brownian motion on the flow of a second-grade liquid over a curved stretching sheet. In Revathi et al. /25/, the ability to increase the rate of absorption in a tray column absorber using methanol-based hybrid nanofluid $CH_3OH+SiO_2+Al_2O_3$ is found.

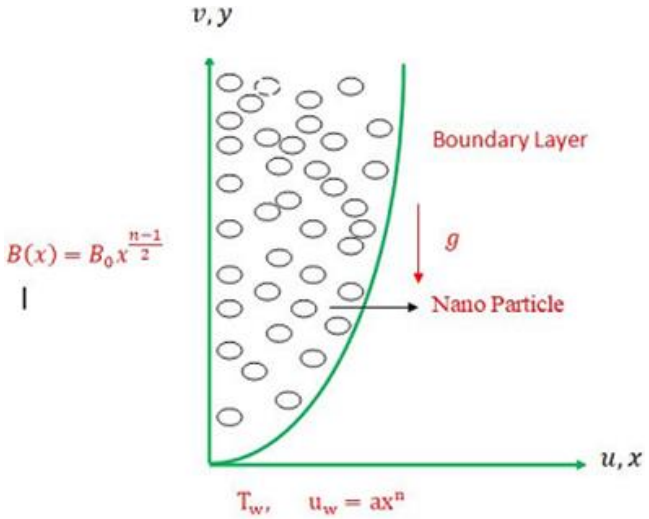

Figure 1. Schematic diagram of the problem.

CONSTRUCTION OF THE PROBLEM

This paper examines a continuous 2-dimensional MHD nanofluid stream across saturated nonlinear stretched sheet in a porous medium when thermal energy and a nonlinear heat source/sink are present. Copper nanoparticles are used with water as the base fluid. It is commonly accepted that the suspended nanoparticles and the base fluid are in thermal equilibrium. Understood to be in the following form are the fluctuating stretching speed, changeable magnetic field and porous medium permeability in the flow of nanofluids $u_w = ax^n$, $B(x) = B_0x^{(n-1)/2}$, $K(x) = K_0x^{1-n}$ correspondingly, where the parameter for stretching a sheet is n, the extending constant a, the permeability constant is K_0, and magnetic field's constant is B_0. The stretched sheet's surface is also maintained at a certain temperature $T_w = T_\infty + bx^{2n-1}\theta$, T_w is the

limitation describing the surface temperature, a constant b (> 0), exist and T_∞ denotes nanofluid's ambient temperature. The flow issue is regulated by the following 2-dimensional continuity, momentum, and energy equations,

$$\frac{\partial u}{\partial x}+\frac{\partial v}{\partial y}=0\,, \tag{1}$$

$$u\frac{\partial u}{\partial x}+v\frac{\partial v}{\partial y}=\frac{\mu_{nf}}{\rho_{nf}}\frac{\partial^2 u}{\partial y^2}-\frac{\sigma_{nf}}{\rho_{nf}}B^2(x)u-\frac{\nu_{nf}}{K(x)}u+g\beta_{nf}(T-T_\infty) \tag{2}$$

$$u\frac{\partial u}{\partial x}+v\frac{\partial v}{\partial y}=\frac{k_{nf}}{(\rho C_p)_{nf}}\frac{\partial^2 T}{\partial y^2}+\frac{q'''}{(\rho C_p)_{nf}}-\frac{1}{(\rho C_p)_{nf}}\frac{\partial q_r}{\partial y}+$$
$$+\frac{\sigma_{nf}}{(\rho C_p)_{nf}}B^2(x)u^2+\frac{\mu_{nf}}{(\rho C_p)_{nf}}\left(\frac{\partial u}{\partial y}\right)^2, \tag{3}$$

with the associated boundary conditions,

$$u=u_w=ax^n,\ v=0,\ T=T_w=T_\infty+bx^{2n-1},\ \text{at}\ y=0$$
$$u\to 0,\ T\to T_\infty\ \text{as}\ y\to\infty\,, \tag{4}$$

where: u and v are the consequent lateral and vertical velocities in the xy-path; x and y are directions parallel to the sheet and along the sheet, respectively; ρ_{nf} is effective density; k_{nf} is thermal conductivity of nanofluids; μ_{nf} is coefficient of viscosity; $K(x)$ is variable permeability; $(\rho C_p)_{nf}$ is the warm capacitance at steady pressure; β_{nf} is thermal expansion, σ_{nf} is electrical conductivity; respectively. Whereas the radioactive warm flux and variable heat source/sink, respectively, are denoted by symbols q_r and q''' and is given by

$$q'''=\frac{k_{nf}u_w}{xv_{nf}}(A^*(T_w-T_\infty)f'+B^*(T-T_\infty))\,. \tag{5}$$

The approximate Rosseland's formula for the radiant heat flow is

$$q_r=-\frac{4}{3}\frac{\sigma^*}{k^*}\frac{\partial T^4}{\partial y}\,, \tag{6}$$

where the Stefan-Boltzmann constant σ^* and mean absorption coefficient k^* are used with their respective values. The Tailor series expansion of T^4 about T_∞ is

$$T^4=4TT_\infty^3-3T_\infty^4\,. \tag{7}$$

Nanofluid's thermophysical characteristics are described as

$$N_1=\frac{\rho_{nf}}{\rho_f}=(1-\phi)+\frac{\rho_s}{\rho_f}\,, \tag{8}$$

$$N_2=\frac{\mu_{nf}}{\mu_f}=\frac{1}{(1-\phi)^{2.5}}\,, \tag{9}$$

$$N_3=\frac{\sigma_{nf}}{\sigma_f}=1+\frac{3\left(\frac{\sigma_s}{\sigma_f}-1\right)\phi}{\left(\frac{\sigma_s}{\sigma_f}+2\right)-\left(\frac{\sigma_s}{\sigma_f}-1\right)\phi}\,, \tag{10}$$

$$N_4=\frac{(k_s+2k_f)-2\phi(k_f-k_s)}{(k_s+2k_f)+\phi(k_f-k_s)}\,, \tag{11}$$

$$N_5=\frac{(\rho C_p)_{nf}}{(\rho C_p)_f}=(1-\phi)+\phi\frac{(\rho C_p)_s}{(\rho C_p)_f}\,, \tag{12}$$

$$N_6=\frac{(\rho\beta)_{nf}}{(\rho\beta)_f}=(1-\phi)+\phi\frac{(\rho\beta)_s}{(\rho\beta)_f}\,, \tag{13}$$

where: ϕ is nanoparticle fraction of solid volume; k_s is the thermal efficiency of nanoparticles; ρ_f is density of the pure fluid; k_f is thermal efficiency of base fluid; ρ_s is nanoparticle density; σ_s, σ_f are conductivity of electricity of nanoparticles and base fluid; μ_f is effective viscosity of base fluid; $(\rho C_p)_s$, $(\rho C_p)_f$ are heat capacitances of nanoparticle and base fluid; β_s, β_f are temperature expansion factors of nanoparticles and base fluid, respectively. The following non-dimensional similarity transformations are introduced for the purpose of simplifying the equations with partial differentials (2) and (3) into equations of ordinary differential types that are not dimensional,

$$\eta=y\sqrt{\frac{(n+1)a}{2\nu}x^{(n-1)/2}},\ \psi=\sqrt{\frac{2\nu a}{n+1}}x^{\frac{n+1}{2}}f(\eta),\ \theta(\eta)=\frac{T-T_\infty}{T_w-T_\infty} \tag{14}$$

where: $\eta(x,y)$ is the likeness variable; ν denotes the fluid's kinematic viscosity. Dimensionless temperature and the stream function specified by $\theta(\eta)$ and $\psi(x,y)$. Velocity components can be defined as follows in terms of the stream function ψ,

$$u=\frac{\partial\psi}{\partial y},\ v=-\frac{\partial\psi}{\partial x}\,. \tag{15}$$

Equations (2) and (3) are changed by putting Eqs.(5)-(15) into them,

$$f'''=\frac{2}{n+1}\left(\frac{N_3}{N_2}M+K\right)f'+\frac{N_1}{N_2}\left(\frac{2n}{n+1}f'^2-ff''\right)-\frac{N_6}{N_2}\frac{2\lambda}{n+1}\theta \tag{16}$$

$$\left(1+\frac{\mathrm{Ra}}{N_4}\right)\theta''=\frac{\mathrm{Pr}}{N_4}\left[N_5\left(\frac{2(2n-1)}{n+1}f'\theta-f\theta'\right)-Ec\left(N_2f''^2+\right.\right.$$
$$\left.\left.+N_3\frac{2m}{n+1}f'^2\right)\right]-\frac{2}{n+1}\frac{N_1}{N_2}(A^*f'+B^*\theta)\,, \tag{17}$$

dependent upon subsequent non-dimensional circumstances

$$f(\eta)=0,\ f'(\eta)=1,\ \theta(\eta)=1,\ \text{at}\ \eta=0$$
$$f'(\eta)=0,\ \theta(\eta)=0,\ \text{as}\ \eta\to\infty\,, \tag{18}$$

where: $M=\frac{\sigma_f B_0^2}{a\rho_f}$ is magnetic restriction; $K=\frac{\nu_f}{aK_0}$ is the porous medium permeability parameter; $\lambda=\frac{\mathrm{Gr}}{\mathrm{Re}^2}$ is mixed convection parameter, where $\mathrm{Gr}=g\beta_f(T_w-T_\infty)\frac{x^3}{\nu_f^2}$ is the Grashof number; and $\mathrm{Re}=\frac{xU_w}{\nu_f}$ is the Reynolds number; $\mathrm{Ra}=\frac{16\sigma^*T_\infty^3}{3k^*k_f}$ is the radiation parameter; $\mathrm{Pr}=\frac{\nu_f(\rho C_p)_f}{k_f}$ is Prandtl number; $\mathrm{Ec}=\frac{U_w^2}{(C_p)_f(T_w-T_\infty)}$ is Eckert number.

The engineering physical parameters are skin friction coefficient C_{fx} and local Nusselt number Nu_x. These are given by:

$$C_{f_x}=\frac{\tau_w}{\rho_f U_w^2},\ \mathrm{Nu}_x=\frac{xq_w}{k_f(T_w-T_\infty)}\,, \tag{19}$$

where

$$\tau_w=\mu_{nf}\left(\frac{\partial u}{\partial y}\right)_{y=0},\ q_w=-k_{nf}\left(\frac{\partial T}{\partial y}\right)_{y=0}+(q_r)_{y=0}\,, \tag{20}$$

the relations will be

$$C_{f_x}\,\mathrm{Re}_x^{1/2} = \frac{1}{(1-\phi)^{2.5}}\left(\frac{n+1}{2}\right)^{1/2} f''(0)\,, \qquad (21)$$

$$\mathrm{Nu}_x\,\mathrm{Re}_x^{-1/2} = -N_4\left(1+\frac{\mathrm{Ra}}{N_4}\right)\left(\frac{n+1}{2}\right)^{1/2}\theta'(0)\cdot \qquad (22)$$

The result of Eqs.(16)-(17) jointly through borderline circumstances Eq.(18) is determined through a systematic numerical method as the shooting technique. We translate the nonlinear equivalences into first order regular differential equivalences by labelling the variable quantity, i.e., $f = f_1$, $f' = f_2$, $f'' = f_3$, $f''' = f_3'$, $\theta = f_4$, $\theta' = f_5$, $\theta'' = f_5'$.

Hence, the system of equations becomes

$$f_1' = f_2,\ f_2' = f_3,\ f_3' = \frac{2}{n+1}\left(\frac{N_3}{N_2}M + K\right) + \frac{N_1}{N_2}\left(\frac{2n}{n+1}f_2^2 - f_1 f_3\right) - \frac{N_6}{N_2}\frac{2\lambda}{n+1}f_4\,, \qquad (23)$$

$$f_4' = f_5,\ f_5' = \left(1+\frac{\mathrm{Ra}}{N_4}\right)^{-1}\left\{\frac{\mathrm{Pr}}{N_4}\left[N_5\left(\frac{2(2n-1)}{n+1}f_2 f_4 - f_1 f_5\right) - \mathrm{Ec}\left(N_2 f_3^2 + N_3\frac{2m}{n+1}f_2^2\right)\right] - \frac{2}{n+1}\frac{N_1}{N_2}(A^* f_2 + B^* f_4)\right\}, \qquad (24)$$

$$f_1(0) = 0,\ f_2(0) = 1,\ f_4(0) = 1,\ \text{as}\ \eta \to 0,$$
$$f_2(\infty) = 0,\ f_4(\infty) = 0,\ \text{as}\ \eta \to 0\,. \qquad (25)$$

The 4th-order Runge-Kutta method combined with a shooting technique is employed for stepwise integration, and calculations are conducted using MATLAB® software.

INFLUENCE OF DIVERSE RESTRICTIONS

In this paper, we use a nanofluid model with a nanoparticle volume fraction to see how a nonlinear stretch sheet affects the stream of a magnetohydrodynamic nanofluid by producing heat, radiating heat, and dissipating heat. Figures 2a and 2b show how the magnetic constraint M affects velocity and temperature. Here, we observed that the temperature increases as M increases, but the velocity profile decreases. It is noteworthy to observe that a stronger magnetic field makes nanofluid flow more difficult. The momentum boundary layer thickness decreases as a result of change in the velocity profile, as illustrated in Fig. 2a. Higher values of M result in a larger Lorentz force in the magnetic field which increases the thickness of the thermal boundary layer.

Table 1. Skin friction coefficient and Nusselt number with respect to parameters M, Pr, K, Fi, λ, Ra, Ec, A^*, B^*, and n.

Parameter	$C_f\mathrm{Re}^{1/2}$	$\mathrm{NuRe}^{-1/2}$
M = 1	-4.312859	-2.419147
M = 2	-4.538491	-2.762798
M = 3	-4.754942	-3.094793
Pr = 4	-4.274883	-2.214479
Pr = 5	-4.312859	-2.419147
Pr = 6	-4.337168	-2.680131
Pr = 7	-4.355598	-2.960463
K = 0	-2.143398	-1.688000
K = 0.25	-3.365953	-2.036332
K = 0.5	-4.312859	-2.419147
K = 1	-5.807584	-3.152316
Fi = 0.5	-4.312859	-2.419147
Fi = 0.55	-5.563274	-2.799610
Fi = 0.6	-7.385978	-3.452175
Fi = 0.65	-10.187514	-4.571075
λ = 1	-4.312859	-2.419147
λ = 2	-3.709127	-2.116945
λ = 3	-3.122402	-1.897445
Ra = 0.1	-4.318104	-2.411620
Ra = 0.5	-4.312859	-2.419147
Ra = 1.5	-4.299615	-2.446785
Ec = 0.2	-4.312859	-2.419147
Ec = 0.5	-4.143767	-5.575018
Ec = 0.8	-3.983659	-8.433959
A^* = –2	-4.437335	-0.831094
A^* = –1	-4.398341	-1.339466
A^* = 0	-4.356642	-1.869702
A^* = 1	-4.312859	-2.419147
B^* = –0.5	-4.395837	-1.486713
B^* = 0	-4.360049	-1.904231
B^* = 0.5	-4.312859	-2.419147
B^* = 1	-4.245589	-3.102538
n = 0.1	-3.676495	-6.170103
n = 0.2	-4.059005	-3.744905
n = 0.3	-4.312859	-2.419147
n = 0.4	-4.515895	-1.501794

Evidently, the Lorentz force is generated by a magnetic field of antagonistic/resistive strength that causes the velocity of the fluid to drop and causes the flow boundary layer to narrow. Moreover, the thickness of the heat boundary layer increases as the temperature profile improves. Figures 3a and 3b show the behaviour of the velocity and the temperature profile for various values of Prandtl number Pr. These data make it abundantly evident that a rise in Pr lowers the velocity and temperature profiles, which leads to a reduction in the thickness of the thermal boundary layer. Figures 3a and 3b depict the velocity and temperature profiles across various values of Prandtl number Pr. The findings reveal a notable decrease in both velocity and temperature profiles with an increase in Pr leading to a reduction in thickness of the thermal boundary layer. The influence of radiation parameter Ra on velocity and temperature profiles is illustrated in Figs. 4a and 4b. Observations indicate a rise in velocity with increasing Ra, while temperature distribution decreases for η = [0, 0.816] and increases for η = [0.816, 8]. Figures 5a and 5b describe the impact of mixed convection parameter λ on velocity and temperature. As λ increases, velocity rises, while temperature decreases. The variation of Eckert number Ec with velocity and temperature profiles is depicted in Figs. 6a and 6b, showcasing an increase in both with higher Ec. The generation of thermal energy intensifies with Ec in the nanofluid, improving temperature distributions and thickening the thermal boundary layer due to frictional heating. Figures 7a and 7b demonstrate the effect of permeability restriction K on the velocity field and temperature distribution. Findings suggest an increase in velocity and a decrease in temperature with amplified K. Figures 8a, 8b, 9a, and 9b highlight the effects of non-uniform heat source/sink parameters (A^*, B^*) on velocity and temperature distributions, both of which increase with higher values of these parameters. Figures 10a and 10b show how velocity and temperature profiles are influenced by the nonlinear stretching sheet parameter n with both decreasing as n increases. Figure 11 illustrates the impact of nanoparticle volume fraction Fi on tem-

perature distribution. Increasing Fi enhances temperature profiles due to improved thermal conductivity, leading to a thickening of the thermal boundary layer.

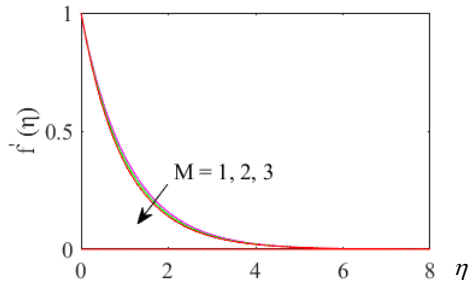

Figure 2a. Velocity $f'(\eta)$ with η for disparate facts of *M*.

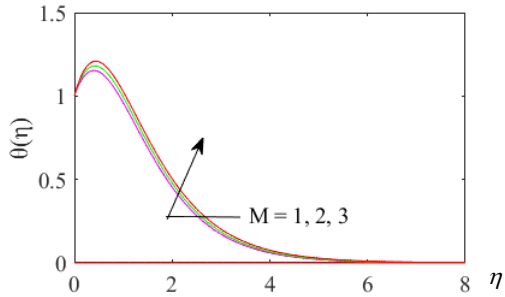

Figure 2b. Temperature $\theta(\eta)$ with η for disparate facts of M.

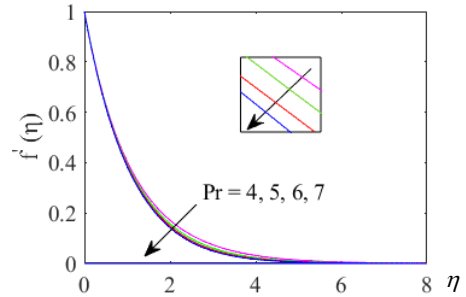

Figure 3a. Velocity $f'(\eta)$ with η for disparate facts of Pr.

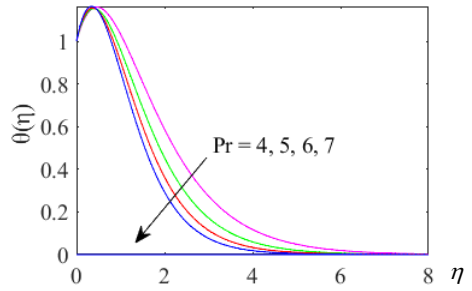

Figure 3b. Temperature with η for disparate facts of Pr.

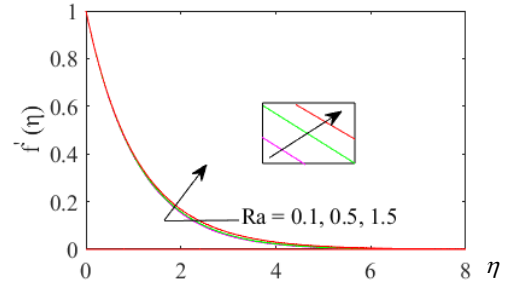

Figure 4a. Velocity $f'(\eta)$ with η for disparate facts of Ra.

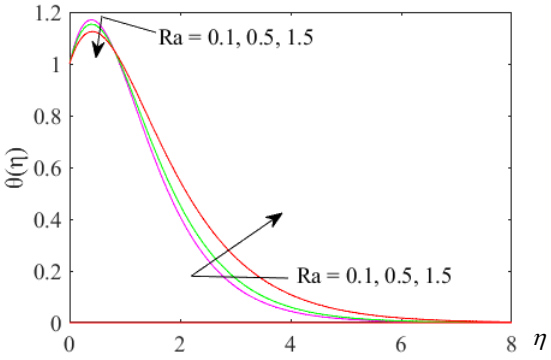

Figure 4b. Temperature with η for disparate facts of Ra.

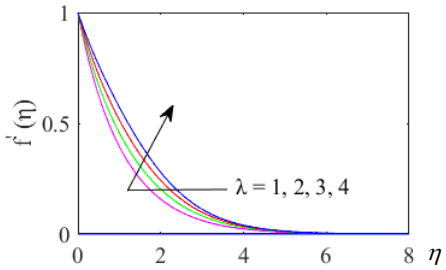

Figure 5a. Velocity $f'(\eta)$ with η for disparate facts of λ.

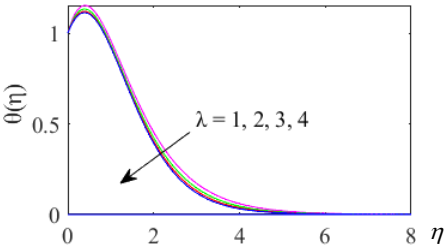

Figure 5b. Temperature with η for disparate facts of λ.

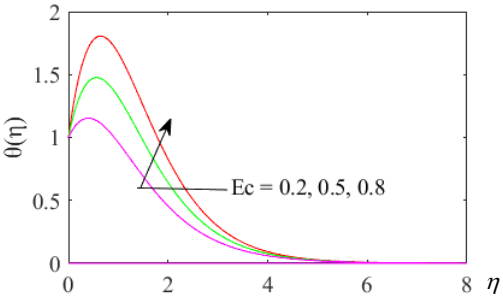

Figure 6a. Velocity $f'(\eta)$ with η for disparate facts of Ec.

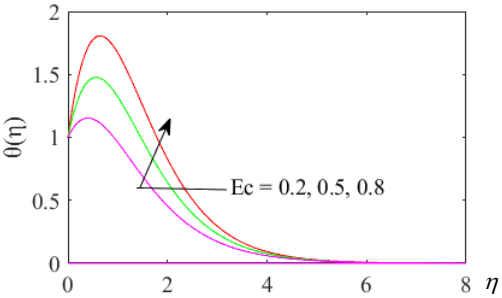

Figure 6b. Temperature with η for disparate facts of Ec.

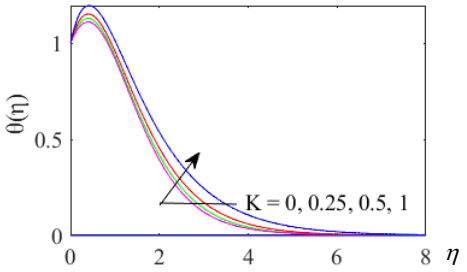

Figure 7a. Velocity $f'(\eta)$ with η for disparate facts of K.

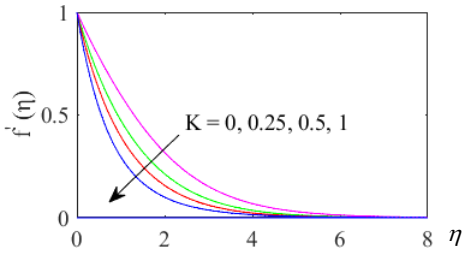

Figure 7b. Temperature $\theta(\eta)$ with η for disparate facts of K.

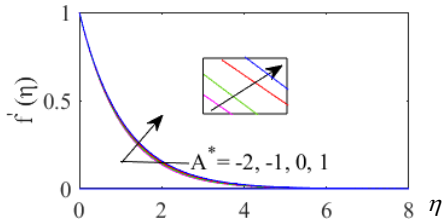

Figure 8a. Velocity $f'(\eta)$ with η for disparate facts of heat source/sink parameter that is not uniform A^*.

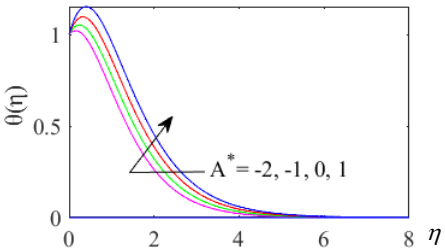

Figure 8b. Temperature $\theta(\eta)$ with η for disparate facts of heat source/sink parameter that is not uniform A^*.

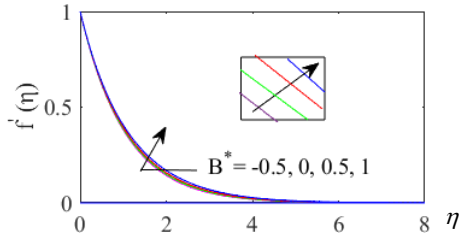

Figure 9a. Velocity $f'(\eta)$ with η for disparate facts of non-uniform heat source/sink parameter B^*.

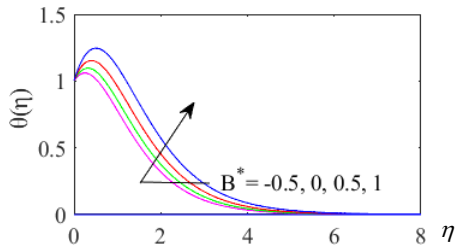

Figure 9b. Temperature $\theta(\eta)$ with η for disparate facts of non-uniform heat source/sink parameter B^*.

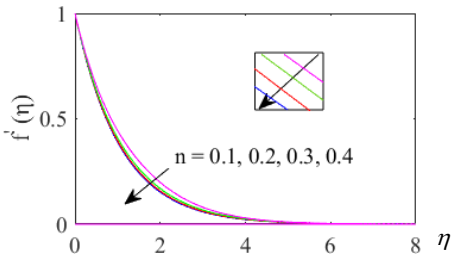

Figure 10a. Velocity $f(\eta)$ with η for disparate facts of n.

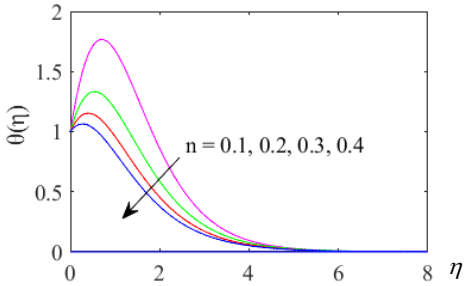

Figure 10b. Temperature θ with η for disparate facts of n.

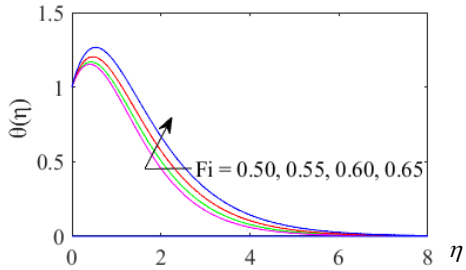

Figure 11. Temperature $\theta(\eta)$ with η for disparate facts of Fi.

CONCLUSIONS

The study explores effects of radiation parameter, non-uniform heat source/sink parameters, nanoparticle volume fraction, and Eckert number on nanofluid magnetohydrodynamic flow over a nonlinear stretching sheet saturated in a porous medium. By employing transformation of similarity, governing partial differential equations governing fluid flow and heat transfer are converted into a system of higher-order ordinary differential equations, which are subsequently solved using the fourth-order Runge-Kutta method. Investigation shows how controlling variables behaviour such as magnetic parameter M, Prandtl numeral Pr, radiation parameter Ra, mixed convection parameter λ, Eckert number Ec, permeability parameter K, non-uniform heat source/sink parameter (A^*, B^*), nonlinear stretching parameter n, and nanoparticle volume fraction Fi, impact parameters of heat transfer issues and nanofluid flow. The study is summarised as follows.

In the region of thermal layer, the temperature distribution and velocity field are enhanced. with an amplify in Eckert number Ec, and the non-uniform heat source/sink parameter (A^*, B^*), while the reverse effect is seen for Prandtl number Pr.

An increase in the value of magnetic parameter M, permeability parameter K, and nonlinear stretching parameter n decreases the velocity field and enhances the temperature distribution while the reverse effect is seen for the mixed convection parameter λ.

Velocity increases with amplified radiation parameter Ra and temperature decreases with amplified radiation parameter Ra for η = [0, 0.816] and increases for η = [0.816, 8].

When volume fraction of nanoparticles Fi rises, temperature rises as well.

The decreasing functions of the magnetic parameter M, Prandtl number Pr, permeability parameter K, and nanoparticle volume fraction Fi are the Nusselt number and skin friction coefficient, while the reverse effect is seen for mixed convection parameter λ.

The coefficient of skin friction is an increasing function and the Nusselt number a decreased function of radiation parameter Ra, non-uniform heat source/sink parameters (A^*, B^*), and Eckert number Ec, while the reverse effect is seen in nonlinear stretching parameter n.

REFERENCES

1. Daniel, Y.S., Aziz, Z.A., Ismail, Z. (2020), *Slip role for unsteady MHD mixed convection of nanofluid over stretching sheet with thermal radiation and electric field*, Ind. J Physics, 94(2): 195-207. doi: 10.1007/s12648-019-01474-y
2. Das, K. (2015), *Nanofluid flow over a non-linear permeable stretching sheet with partial slip*, J Egypt. Math. Soc. 23(2): 451-456. doi: 10.1016/j.joems.2014.06.014
3. Das, K., Sarkar, A., Kundu, P.K. (2017), *Cu-water nanofluid flow induced by a vertical stretching sheet in presence of a magnetic field with convective heat transfer*, Propul. Power Res. 6(3): 206-213. doi: 10.1016/j.jppr.2017.07.001
4. Devi, S.U., Devi, S.P.A. (2017), *Heat transfer enhancement of Cu-Cl_2O_3/water hybrid nanofluid flow over a stretching sheet*, J Niger. Math. Soc. 36(2): 419-433.
5. Faraz, F., Haider, S., Imran, S.M. (2020), *Study of magneto-hydrodynamics (MHD) impacts on an axisymmetric Casson nano-fluid flow and heat transfer over unsteady radially stretching sheet*, SN Appl. Sci. 2: 14. doi: 10.1007/s42452-019-1785-5
6. Geng, Y., Hassanvand, A., Monfared, M., Moradi, R. (2019), *MHD nanofluid heat transfer between a stretching sheet and a porous surface using neural network approach*, Int. J Modern Phys. C, 30(06): 1950048.1. doi: 10.1142/S0129183119500487
7. Goyal, M., Bhargava, R. (2014), *Boundary layer flow and heat transfer of viscoelastic nanofluids past a stretching sheet with partial slip conditions*, Appl. Nanosci. 4(6): 761-767. doi: 10.1007/s13204-013-0254-5
8. Haroun, N.A.H., Mondal, S., Sibanda, P. (2019), *Hydromagnetic nanofluids flow through a porous medium with thermal radiation, chemical reaction and viscous dissipation using the spectral relaxation method*, Int. J Comput. Meth. 16(06): 1840020. doi: 10.1142/S0219876218400200
9. Hayat, T., Khan, W.A., Abbas, S.Z., et al. (2020), *Impact of induced magnetic field on second-grade nanofluid flow past a convectively heated stretching sheet*, Appl. Nanosci. 10(8): 3001-3009. doi: 10.1007/s13204-019-01215-x
10. Hayat, T., Nadeem, S. (2017), *Heat transfer enhancement with Ag-CuO/water hybrid nanofluid*, Results in Phys. 7: 2317-2324. doi: 10.1016/j.rinp.2017.06.034
11. Jamaludin, A., Nazar, R., Pop, I. (2018), *Three-dimensional magnetohydrodynamic mixed convection flow of nanofluids over a nonlinearly permeable stretching/shrinking sheet with velocity and thermal slip*, Appl. Sci. 8(7): 1128. doi: 10.3390/app8071128
12. Khan, J.A., Mustafa, M., Hayat, T., Alsaedi, A. (2015), *Three-dimensional flow of nanofluid over a non-linearly stretching sheet: An application to solar energy*, Int. J Heat Mass Transf. 86: 158-164. doi: 10.1016/j.ijheatmasstransfer.2015.02.078
13. Khan, M., Azam, M. (2017), *Unsteady heat and mass transfer mechanisms in MHD Carreau nanofluid flow*, J Molec. Liq. 225: 554-562. doi: 10.1016/j.molliq.2016.11.107
14. Khan, S.A., Nie, Y., Ali, B. (2020), *Multiple slip effects on MHD unsteady viscoelastic nano-fluid flow over a permeable stretching sheet with radiation using the finite element method*, SN Appl. Sci. 2(1): 66. doi: 10.1007/s42452-019-1831-3
15. Khan, W., Pop, I. (2010), *Boundary-layer flow of a nanofluid past a stretching sheet*, Int. J Heat Mass Transf. 53(11-12): 2477-2483. doi: 10.1016/j.ijheatmasstransfer.2010.01.032
16. Mabood, F., Yusuf, T.A., Khan, W.A. (2021), *Cu-Al_2O_3-H_2O hybrid nanofluid flow with melting heat transfer, irreversibility analysis and nonlinear thermal radiation*, J Therm. Anal. Calorim. 143(2): 973-984. doi: 10.1007/s10973-020-09720-w
17. Malvandi, A., Hedayati, F., Ganji, D.D. (2018), *Nanofluid flow on the stagnation point of a permeable non-linearly stretching/shrinking sheet*, Alex. Eng. J, 57(4): 2199-2208. doi: 10.1016/j.aej.2017.08.010
18. Nandeppanavar, M.M., Vaishali, S., Kemparaju, M.C., Raveendra, N. (2020), *Theoretical analysis of thermal characteristics of casson nano fluid flow past an exponential stretching sheet in Darcy porous media*, Case Studies Therm. Eng. 21: 100717. doi: 10.1016/j.csite.2020.100717
19. Naramgari, S., Sulochana, C. (2016), *Dual solutions of radiative MHD nanofluid flow over an exponentially stretching sheet with heat generation/absorption*, Appl. Nanosci. 6(1): 131-139. doi: 10.1007/s13204-015-0420-z
20. Naveen Kumar, R., Suresha, S., Gowda, R.J.P., et al. (2021), *Exploring the impact of magnetic dipole on the radiative nanofluid flow over a stretching sheet by means of KKL model*, Pramana - J Phys. 95(4): 180. doi: 10.1007/s12043-021-02212-y
21. Pal, D., Mandal, G. (2015), *Mixed convection-radiation on stagnation-point flow of nanofluids over a stretching/shrinking sheet in a porous medium with heat generation and viscous dissipation*, J Petrol. Sci. Eng. 126: 16-25. doi: 10.1016/j.petrol.2014.12.006
22. Patel, H.R. (2019), *Effects of cross diffusion and heat generation on mixed convective MHD flow of Casson fluid through porous medium with non-linear thermal radiation*, Heliyon, 5(4): e01555. doi: 10.1016/j.heliyon.2019.e01555
23. Punith Gowda, R.J., Baskonus, H.M., Naveen Kumar, R., et al. (2021), *Computational investigation of Stefan blowing effect on flow of second-grade fluid over a curved stretching sheet*, Int. J Appl. Comput. Math. 7(3): 109. doi: 10.1007/s40819-021-01041-2
24. Rana, P., Bhargava, R. (2012), *Finite element simulation of transport phenomena of viscoelastic nanofluid over a stretching sheet with energy dissipation*, J Inform. Oper. Manag. 3(1): 158-161.
25. Revathi, G., Sajja, V.S., Babu, M.J., et al. (2023), *Entropy optimization in hybrid radiative nanofluid (CH_3OH+SiO_2+Al_2O_3) flow by a curved stretching sheet with cross-diffusion effects*, Appl. Nanosci. 13: 337-351. doi: 10.1007/s13204-021-01679-w
26. Roy, N.C., Pop, I. (2020), *Flow and heat transfer of a second-grade hybrid nanofluid over a permeable stretching/shrinking sheet*, The Europ. Phys. J Plus, 135(9): 768. doi: 10.1140/epjp/s13360-020-00788-9
27. Sandeep, N., Sulochana, C., Raju, C.S.K., et al. (2015), *Unsteady boundary layer flow of thermophoretic MHD nanofluid past a stretching sheet with space and time dependent internal heat source/sink*, Applic. Appl. Math.: An Int. J, 10(1): 20.
28. Xuan, Y., Li, Q. (2000), *Heat transfer enhancement of nanofluids*, Int. J Heat Fluid Flow, 21(1): 58-64. doi: 10.1016/S0142-727X(99)00067-3
29. Zeeshan, A., Ellahi, R., Hassan, M. (2014), *Magnetohydrodynamic flow of water/ethylene glycol based nanofluids with natural convection through a porous medium*, Eur. Phys. J Plus, 129(12): 261. doi: 10.1140/epjp/i2014-14261-5